

## A New Highly Selective Fluorescent K<sup>+</sup> Sensor

Xianfeng Zhou,<sup>†</sup> Fengyu Su,<sup>†</sup> Yanqing Tian,<sup>\*</sup> Cody Youngbull, Roger H. Johnson, and Deirdre R. Meldrum

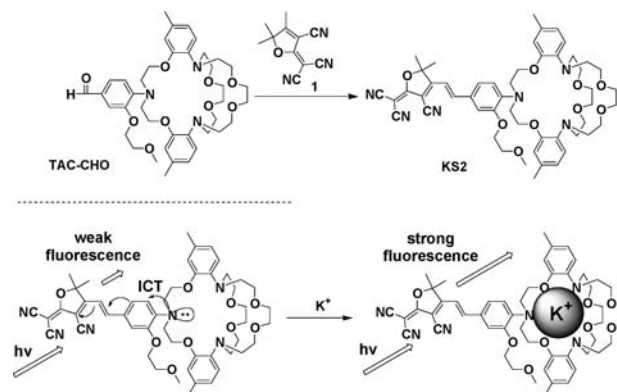
Center for Biosignatures Discovery Automation, Biodesign Institute, Arizona State University, Tempe, Arizona 85287, United States

**S** Supporting Information

**ABSTRACT:** We describe the synthesis, properties, and application of a new fluorescent potassium chemosensor, KS2, for K<sup>+</sup> sensing and imaging in live cells. By virtue of a strong electron-withdrawing group, 2-dicyanomethylene-3-cyano-4,5,5-trimethyl-2,5-dihydrofuran (TCF), with a triazacryptand ligand, the new sensor can respond to K<sup>+</sup> up to 1.6 M. This is the first highly selective intracellular sensor suitable for sensing K<sup>+</sup> over a broad and high concentration range. Confocal fluorescence microscopy has established the utility of KS2 for live-cell K<sup>+</sup> detection. The application of KS2 combined with other sensors will be of great benefit for investigating cellular metabolism, detecting and diagnosing diseases including cancer, and monitoring responses to therapy.

Potassium makes up about 0.4% of the mass in the human body and is the most abundant intracellular cation. Potassium ions (K<sup>+</sup>) play diverse roles in biological processes including muscle contraction, heartbeat, nerve transmissions, and kidney functions. Abnormal K<sup>+</sup> fluctuations are early indicators of diseases such as alcoholism, anorexia, bulimia, heart disease, diabetes, AIDS, and cancer.<sup>1</sup> Confocal fluorescence microscopy has proven to be an important tool in understanding metal ion biology<sup>2</sup> and has the potential to measure changes in K<sup>+</sup> concentrations with high spatial and temporal fidelity. One of the earliest and best-known intracellular fluorescent K<sup>+</sup> probes is potassium-binding benzofuran isophthalate (PBFI), which uses a diaz-18-crown-6 as a ligand and a benzofuran derivative as the fluorophore. PBFI, however, suffers poor selectivity with respect to sodium ions (Na<sup>+</sup>).<sup>3</sup> To alleviate this problem, He et al.<sup>3</sup> developed a ligand based on a triazacryptand (TAC) platform, which features excellent selective responses for K<sup>+</sup> over competing sodium ions. Verkman's group developed other fluorescent K<sup>+</sup> sensors based on this ligand.<sup>4–6</sup> He et al. and Verkman et al. chemically grafted their K<sup>+</sup> probes onto biocompatible polymers for extracellular K<sup>+</sup> sensing. Physiological extracellular K<sup>+</sup> concentrations are around 5 mM,<sup>7</sup> while cells usually contain about 150 mM intracellular K<sup>+</sup>.<sup>8</sup> Erythrocytes and epidermal cells contain more intracellular K<sup>+</sup>, with homeostasis concentrations of 200 and 475 mM, respectively.<sup>8</sup> For myocytes, the intracellular K<sup>+</sup> concentration is even higher, at molar levels.<sup>8</sup> Therefore, ideal intracellular K<sup>+</sup> sensors should be applicable for measurements of high K<sup>+</sup> concentrations with a relatively large dissociation constant (*K*<sub>d</sub>) (e.g., around 100 mM). Commercially available PBFI has a millimolar *K*<sub>d</sub> (6.6 mM),<sup>9</sup> which is not ideal for highly concentrated intracellular K<sup>+</sup> sensing. Although the *K*<sub>d</sub> values for the K<sup>+</sup> sensors possessing the TAC ligands were not reported,

Scheme 1. Synthesis of KS2 and Its Sensing Mechanism



they could be estimated to be close to that for PBFI on the basis of the results published by He et al.<sup>3</sup> and Verkman et al.<sup>4–6</sup>

Herein we report the new red-fluorescent potassium ion sensor KS2 (Scheme 1). The sensor was constructed using a strong electron-withdrawing group, 2-dicyanomethylene-3-cyano-4,5,5-trimethyl-2,5-dihydrofuran (TCF), and an electron-donating group, an aniline derivative of the TAC ligand for K<sup>+</sup> sensing. TCF has been known as a strong acceptor and was initially used for nonlinear optical materials<sup>10,11</sup> and later for red fluorophores for bioimaging<sup>12,13</sup> and pH sensing.<sup>14</sup> Because of the strong delocalization of electrons in the push–pull fluorophore in KS2, the complexing ability of the nitrogen atom of the aniline group, a component of the ligand for the potassium ion, decreased significantly. Such a decrease may result in a blunted binding ability of the whole ligand in KS2 and decreased sensitivity of the intramolecular charge transfer (ICT) to the complexation with K<sup>+</sup>, resulting in a *K*<sub>d</sub> of around 0.1 M.

KS2 was constructed using strong electron-donating (aniline) and electron-withdrawing (TCF) groups, yielding an absorption maximum at 560 nm. The extinction coefficient ( $\epsilon$ ) at 560 nm is  $3.84 \times 10^4 \text{ M}^{-1} \text{ cm}^{-1}$  (S-Figure 1 and S-Table 1 in the Supporting Information). KS2 displays weak fluorescence in its free form, with a quantum yield ( $\eta$ ) of 0.11%. Upon addition of K<sup>+</sup>, the fluorescence intensity of KS2 increases by around 4- and 50-fold at K<sup>+</sup> concentrations of 140 and 1400 mM, respectively (Figure 1a,b), resulting in corresponding  $\eta$  values of 0.52% and 5.6% (S-Table 1). *K*<sub>d</sub> was determined by the Benesi–Hildebrand equation (eq 1),<sup>15</sup>

$$\frac{F_0}{F_0 - F} = \frac{F_0}{F_0 - F_{\text{complex}}} + \frac{F_0}{F_0 - F_{\text{complex}}} \cdot K_d \cdot \frac{1}{[\text{M}]} \quad (1)$$

Received: August 4, 2011

Published: October 25, 2011

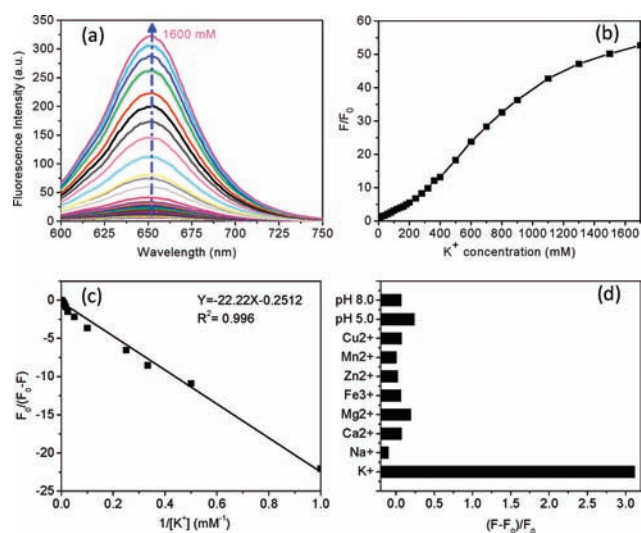


**Figure 1.** (a) Fluorescence change of KS2 in HEPES buffer (pH 7.2) containing different KCl concentrations, excited at 561 nm. (b) Changes of fluorescence intensities at 650 nm at different  $K^+$  concentrations.  $F$  is the fluorescence intensity at various conditions, and  $F_0$  is the emission intensity before the titration (with 0 mM  $K^+$ ). (c) Benesi–Hildebrand plot for KS2. (d) Fluorescence intensity change of KS2 in the presence of various biological cations at their physiological concentrations [ $K^+$  (150 mM),  $Na^+$  (15 mM),  $Ca^{2+}$  (2.0 mM),  $Mg^{2+}$  (2.0 mM),  $Zn^{2+}$  (2.0 mM),  $Fe^{3+}$  (50  $\mu$ M),  $Mn^{2+}$  (50  $\mu$ M), and  $Cu^{2+}$  (50  $\mu$ M)] and different pH values (5.0 and 8.0).

where  $F_0$  is the integrated fluorescence intensity of a free sensor,  $F$  is the observed integrated fluorescence intensity,  $F_{\text{complex}}$  is the emission of the ligand–metal ion complex, and  $[M]$  is the metal ion concentration. When  $F_0/(F_0 - F)$  is plotted against  $1/[M]$ , the binding constant is given by the intercept/slope ratio. From curve fitting of the KS2 fluorescence intensity against the reciprocal of the  $K^+$  concentration ( $1/[K^+]$ ), this Benesi–Hildebrand plot yielded a linear fit (Figure 1c), from which the  $K_d$  value was estimated to be 88 mM. The linear fit evidenced 1:1 complexation behavior.

The KS2 was tested against physiological concentration levels of the following metal ions:  $K^+$ ,  $Na^+$ ,  $Ca^{2+}$ ,  $Mg^{2+}$ ,  $Fe^{3+}$ ,  $Zn^{2+}$ ,  $Mn^{2+}$ , and  $Cu^{2+}$ . The results revealed that the potassium ion had the greatest influence on the sensor's emissions (Figure 1d). Furthermore, this trend was also present when the concentrations of  $Na^+$ ,  $Ca^{2+}$ , and  $Mg^{2+}$  were increased to 140 mM (S-Figure 2). These results showed the high selectivity of KS2 for  $K^+$ . KS2 was not sensitive to pH over the range 5–8. The high selectivity for  $K^+$  with a large  $K_d$  suggested that KS2 might be useful for intracellular  $K^+$  sensing over a wide range of biological conditions.

The cytotoxicity of KS2 to human glioblastoma U87MG cells was studied using Trypan blue staining. After internalization of the sensor with cells for 2 h, more than 97% of the cells were viable, showing the noncytotoxicity of KS2 toward the U87MG cell line under our experimental conditions. Confocal images of U87MG cells internalized with KS2 showed that KS2 could be taken up by cells within 10 min. Red fluorescence was observed in the cytoplasm area, which was further confirmed by a minimum colocalization with blue emission from the nucleic staining probe (Hoechst 33342) (Figure 2). Furthermore, the sensor did not have a specific colocalization in mitochondria or lysosomes,

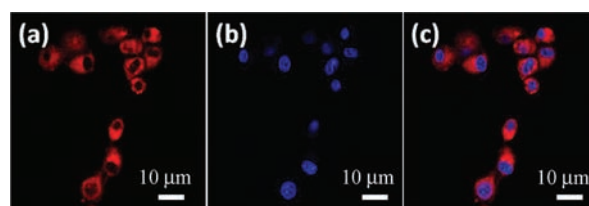


**Figure 2.** Confocal fluorescence images of KS2 (4  $\mu$ M) in U87MG cells costained with Hoechst 33342 (10  $\mu$ M): (a) red emission from KS2 excited at 561 nm; (b) blue emission from Hoechst 33342 excited at 405 nm; (c) overlay of (a) and (b).

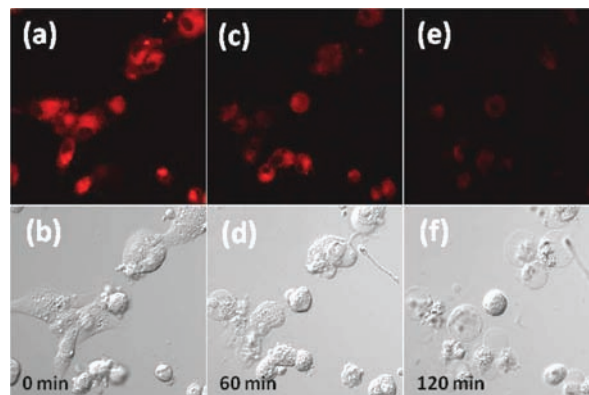


**Figure 3.** Time-dependent intracellular  $K^+$  in U87MG cells after treatment with a mixture of nigericin, bumetanide, and ouabain for (a, b) 0, (c, d) 60, and (e, f) 120 min: (top) fluorescence images; (bottom) bright-field images. The concentrations of KS2, nigericin, bumetanide, and ouabain for this study were 4, 5, 10, and 10  $\mu$ M, respectively. A more detailed time dependence is given in S-Figure 7.

showing that KS2 has a nonspecific distribution and therefore can be used to monitor potassium ions in the cytoplasm and in any of these compartments (S-Figures 4 and 5).

To monitor the stimulus response of the intracellular  $K^+$  level, cells internalized with 4  $\mu$ M KS2 for 10 min were treated with a mixture of nigericin, bumetanide, and ouabain at 37  $^{\circ}$ C (Figure 3). The decrease in the fluorescence intensities indicated the efflux of the intracellular  $K^+$  from cells (Figure 3a,c,e). The combination of the ionophore nigericin with the influx inhibitors bumetanide (inhibitor of  $Na^+$ ,  $K^+$ ,  $2Cl^-$  cotransport) and ouabain (inhibitor of  $Na^+$ ,  $K^+$ , ATPase pump) is an effective  $K^+$  efflux stimulator.<sup>16</sup> This mixture effectively induced  $K^+$  efflux, as shown in fluorescence images (Figure 3). Meanwhile, cell shrinkage with a preservation of an intact plasma membrane was observed after 60 min of stimulation. It has been known that depletion of intracellular  $K^+$  results in cell shrinkage, activated caspases, and DNA fragmentation, all of which are features of apoptosis.<sup>16,17</sup> Therefore, the phenomenon observed in Figure 3 indicated that U87MG cells underwent the apoptotic change through the  $K^+$  efflux induced by nigericin, ouabain, and bumetanide. A control experiment without the drug stimulation showed neither obvious fluorescence intensity changes nor morphological shrinkages (S-Figure 8).

KS2 can also be used to monitor  $K^+$  influx in response to stimuli. Cells internalized with 4  $\mu$ M KS2 for 10 min were treated with 20 mM KCl in medium at 37  $^{\circ}$ C for 1 h. This just induced a slight fluorescence intensity increase (data not shown), whereas

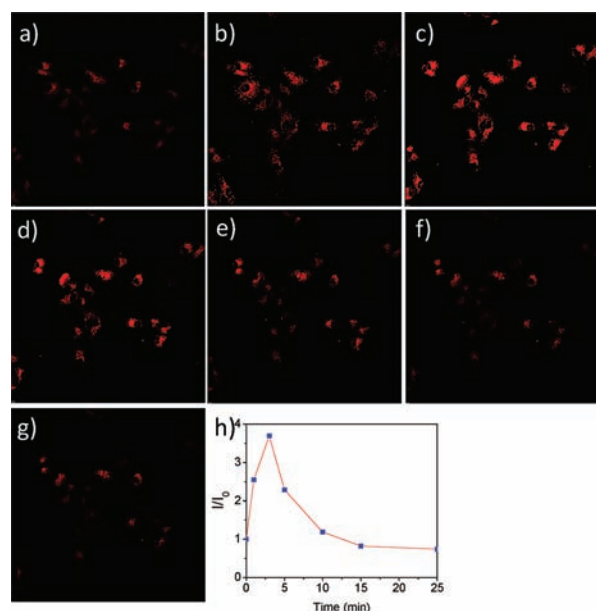


**Figure 4.** (a–g) Time-dependent fluorescence of U87MG cells stimulated by nigericin and observed under confocal fluorescence microscope: (a)  $t = 0$  (before the addition of nigericin); (b–g)  $t = 1, 3, 5, 10, 15,$  and  $25$  min, respectively, after the addition of nigericin ( $20 \mu\text{M}$  final concentration) into the  $20 \text{ mM}$  KCl-containing medium. (h) Average fluorescence intensity ratios as measured by ImageJ.  $I_0$  is the average fluorescence intensity from (a);  $I$  is the average fluorescence intensity at other times. An enlarged version of this figure is shown in S-Figure 10.

an obvious fluorescence increase was observed after the cells were treated with  $5 \mu\text{M}$  isoproterenol and  $20 \text{ mM}$  KCl in medium for  $40 \text{ min}$  at  $37 \text{ }^\circ\text{C}$  (S-Figure 9). Isoproterenol has been reported to stimulate potassium ion influx by stimulating cyclic adenosine monophosphate (cAMP) generation, which is associated with a physiological change in  $\text{K}^+$  transport.<sup>18</sup> The average fluorescence intensity of cells after the treatment was 33% greater than that before the treatment, as quantified using ImageJ software (public domain software developed at the National Institutes of Health).<sup>19</sup>

The sensor was further demonstrated for in situ observation of dynamic potassium ion influx and then efflux through changes in fluorescence stimulated by an ionophore nigericin (Figure 4). Cells internalized with  $4 \mu\text{M}$  KS2 at  $37 \text{ }^\circ\text{C}$  for  $10 \text{ min}$  were washed with  $20 \text{ mM}$  KCl-containing fresh medium. Nigericin ( $20 \mu\text{M}$  at its final concentration) in  $20 \text{ mM}$  KCl-containing medium was added to help  $\text{K}^+$  to cross cell membrane. Enhanced fluorescence was immediately observed after the addition of nigericin, indicating that potassium ion influx occurred. The potassium influx peaked after  $3 \text{ min}$  with an average fluorescence increase of 370%. After  $3 \text{ min}$ , potassium efflux was observed through a decrease in the fluorescence. The efflux stabilized after  $15 \text{ min}$ , and the fluorescence intensity after the stabilization was about 25% below that before the stimulation by nigericin. The ionophore nigericin was used to stimulate  $\text{K}^+$  influx for yeast *Saccharomyces cerevisiae*.<sup>20</sup> It was also reported to be a  $\text{K}^+$  efflux stimulator for human colorectal adenocarcinoma HT-29 cells.<sup>4</sup> The observation of the  $\text{K}^+$  influx and then efflux of U87MG cells using KS2 demonstrates its further utility in measuring the kinetics of  $\text{K}^+$  transport.

In summary, we have described the synthesis, properties, and cellular application of KS2, a new fluorescent chemosensor for  $\text{K}^+$  sensing and imaging. As a result of the inclusion of the strong electron-withdrawing group TCF with the TAC ligand, the new sensor can respond to  $\text{K}^+$  over a broad concentration range up to  $1600 \text{ mM}$ . This is the first highly selective intracellular  $\text{K}^+$  sensor that is capable of being used over such a broad range for highly concentrated  $\text{K}^+$  sensing. Moreover, confocal microscopy experiments established that KS2 can be used for detecting  $\text{K}^+$  levels within living cells. The application of KS2 combined with other sensors for cellular metabolism investigations and disease/cancer detection and diagnosis is underway.

## ■ ASSOCIATED CONTENT

**S Supporting Information.** Synthesis, characterization, and experimental details. This material is available free of charge via the Internet at <http://pubs.acs.org>.

## ■ AUTHOR INFORMATION

### Corresponding Author

yanqing.tian@asu.edu

### Author Contributions

<sup>†</sup>These authors contributed equally.

## ■ ACKNOWLEDGMENT

Financial support was provided by the Microscale Life Sciences Center, an NIH Center of Excellence in Genomic Sciences at Arizona State University (Grant 5P50 HG002360; D.R.M. is the director and principal investigator).

## ■ REFERENCES

- (1) *Potassium Ion Channels: Molecular Structure, Function, and Diseases*; Kurachi, Y., Jan, L. Y., Lazdunski, M., Eds.; Current Topics in Membranes, Vol. 46; Academic Press: San Diego, CA, 1999.
- (2) Taki, M.; Wolford, J. L.; O'Halloran, T. V. *J. Am. Chem. Soc.* **2004**, *126*, 712–713.
- (3) He, H.; Mortellaro, M. A.; Leiner, M. J. P.; Fraatz, R. J.; Tusa, J. K. *J. Am. Chem. Soc.* **2003**, *125*, 1468–1469.
- (4) Namkung, W.; Padmawar, P.; Mills, A. D.; Verkman, A. S. *J. Am. Chem. Soc.* **2008**, *130*, 7794–7795.
- (5) Namkung, W.; Song, Y.; Mills, A. D.; Padmawar, P.; Finkbeiner, W. E.; Verkman, A. S. *J. Biol. Chem.* **2009**, *284*, 15916–15926.
- (6) Padmawar, P.; Yao, X.; Bloch, O.; Manley, G. T.; Verkman, A. S. *Nat. Methods* **2005**, *2*, 825–827.
- (7) Burnell, J. M.; Scribner, B. H.; Uyeno, B. T.; Villamil, M. F. *J. Clin. Invest.* **1956**, *35*, 935–939.
- (8) Sachs, J. R.; Welt, L. G. *J. Clin. Invest.* **1967**, *46*, 65–76.
- (9) Kowalczyk, A.; Boens, N.; Meuwis, K.; Ameloot, M. *Anal. Biochem.* **1997**, *245*, 28–37.
- (10) Gopalan, P.; Katz, H. E.; McGee, D. J.; Erben, C.; Zielinski, T.; Bousquet, D.; Muller, D.; Grazul, J.; Olsson, Y. *J. Am. Chem. Soc.* **2004**, *126*, 1741–1747.
- (11) Liao, Y.; Bhattacharjee, S.; Firestone, K. A.; Eichinger, B. E.; Paranj, R.; Anderson, C. A.; Robinson, B. H.; Reid, P. J.; Dalton, L. R. *J. Am. Chem. Soc.* **2006**, *128*, 6847–6853.
- (12) Lord, S. J.; Conley, N. R.; Lee, H.-I. D.; Samuel, R.; Liu, N.; Twieg, R. J.; Moerner, W. E. *J. Am. Chem. Soc.* **2008**, *130*, 9204–9205.
- (13) Bouffard, J.; Kim, Y.; Swager, T. M.; Weissleder, R.; Hilderbrand, S. A. *Org. Lett.* **2008**, *10*, 37–40.
- (14) Jin, Y.; Tian, Y.; Zhang, W.; Jang, S.-H.; Jen, A. K.-Y.; Meldrum, D. R. *Anal. Bioanal. Chem.* **2010**, *398*, 1375–1384.

- (15) Benesi, H. A.; Hildebrand, J. H. *J. Am. Chem. Soc.* **1949**, *71*, 2703–2707.
- (16) Andersson, B.; Janson, V.; Behnam-Motlagh, P.; Henriksson, R.; Grankvist, K. *Toxicol. In Vitro* **2006**, *20*, 986–994.
- (17) Hughes, F. M., Jr.; Bortner, C. D.; Purdy, G. D.; Cidowski, J. A. *J. Biol. Chem.* **1997**, *272*, 30567–30576.
- (18) Furukawa, H.; Bilezikian, J. P.; Loeb, J. *Biochim. Biophys. Acta* **1980**, *598*, 345–356.
- (19) Collins, T. J. *BioTechniques* **2007**, *43* (Suppl. 1), 25–30.
- (20) Eilam, Y. *J. Gen. Microbiol.* **1982**, *128*, 2611–2614.